LSTM-ANN based DTC of Induction Motor with 5 Level Inverter

Satendra Singh, A Kannagi, Laxmi Goswami and Dhananjay Kumar Yadav

Satendra Singh, Assistant Professor, Mechanical Engineering, Vivekananda Global University, Jaipur, India, Email Id-singh.satendra@vgu.ac.in
A Kannagi, Associate Professor, Department of Computer Science and Information Technology, Jain (Deemed to be University), Bangalore, India, Email Id- a.kannagi@jainuniversity.ac.in
Ms.LaxmiGoswami, Assistant Professor, Department of Electrical Engineering, Sanskriti University, Mathura, Uttar Pradesh, India, Email Id- laxmigoswami.ee@sanskriti.edu.in
Dhananjay Kumar Yadav, Assistant Professor, Maharishi School of Engineering & Technology, Maharishi University of Information Technology, Uttar Pradesh, India, Email Id- dhananjay.rishabh@gmail.com

Abstract: Medium voltage drives especially induction motor drives are mostly using in industries for many applications. The precious intelligent control of induction motors are high required in nuclear power generation units. Direct torque control (DTC) of induction motors is commonly selected for achieving smooth speed torque characteristics as compared with other existing control techniques. However, conventional DTC suffers from many issues because of maintaining constant reference flux in all the speed regions. Hence two ANN controllers based novel DTC is implemented in this paper. Three phase five level neutral point clamped (5L-NPC) inverter is used to drive the induction motor. The dc-link is established through 36 pulse rectifier. Moreover, photovoltaic (PV) system along with battery bank is also integrated to provide continuous power supply during off grid. An unchanging dc-link voltage is achieved by utilizing a bidirectional dc-dc circuit that is connected between the dc-link and the battery. The proposed control of dc-dc bidirectional circuit can further reduce the ripples and oscillations in dc-link produced by 36 pulse rectifier during unbalanced grid voltages. Realistic responses are presented in this paper by establishing hardware – in the – loop (HIL) with the help of OPAL-RT modules. The HIL based results are discussed under various case studies in this paper.

Keywords: Medium voltage drives, DTC, Induction motor, Multilevel inverter, PV, LSTM controller.

Corresponding Author: singh.satendra@vgu.ac.in

© The Authors, published by EDP Sciences. This is an open access article distributed under the terms of the Creative Commons Attribution License 4.0 (https://creativecommons.org/licenses/by/4.0/).

1. INTRODUCTION

Electrical drives are commonly used for multiple applications in industries. Medium voltage drives employed with Multilevel Voltage Source Inverter (MVSI) are more popular due to high reliability and low harmonic distortion. Among different configurations, three phase five level neutral point clamped inverter (5L-NPC) is more suitable to use in nuclear power stations for driving an induction motor [1]. In the other hand, Direct Torque Control (DTC) can have facilities of fast changing torque and flux references, high efficiency, minimum switching losses, no overshoot during step response and instantaneously control the flux and torque in a decoupled way. Therefore implementation of DTC on 5L-NPC inverter can provide a better solution in nuclear power plant. Generally a proportional plus integral (PI) controller is used to obtain reference torque by comparing motor speed with its reference speed and keeping flux at a constant value (i.e. considered constant flux reference). However, to achieve smooth operation during transient periods also, the reference flux needs to be varying according to changes in speed within the limit. Further, fuzzy controllers can exhibits superior performance than PI due to ability of automatic adjustable gains [2]. A LSTM controller is more suitable as compared with fuzzy during random variations of input reference due to its fast ability with less number of rules [3-4]. Hence, two LSTM controllers based DTC of induction motor is implemented with 5L-NPC in this paper.

A 36 pulse diode rectifier is used to provide stable dc-link voltage of the inverter. However, to minimize consumption power from utility grid as well as to provide reliable power to the drive, a PV along with battery is integrated to dc-link. A dc-dc bidirectional circuit is employed between battery and dc-link to maintain charging and discharging process of the battery bank. Further, the control of the dc-dc converter is designed in such a fashion that to minimize oscillation in dc-link due to unbalanced voltages of the grid. Generally second frequency oscillations will be present in voltage dc-link during unbalanced supply voltages in grid. These oscillations further crates shaking affect on shaft of the induction motor which results decreases the fatigue life. Therefore the bidirectional dc-dc converter can help to maintain stable voltage at dc-link irrespective of solar irradiance, unbalances in grid voltages even during off grid.

After achieving a steady voltage at the dc-link, the speed of the induction motor at its setpoint can be easily regulated by a 5L-NPC DTC. However, a Space Vector Pulse Width Modulation (SVPWM) technique can further help to reduce injected harmonics into motor as well as to achieve quick response by selecting the best sector according to requirement. Unfortunately the combinations of vectors are increasing by increasing the level of the multilevel inverter. Therefore, an optimization method is necessary to quickly determine the correct vector for generating the desired output voltage using the inverter. Therefore Modified Invasive Weed Optimization (MIWO) technique is developed to identify correct voltage sector quickly for generating required pulses to the 5L-NPC inverter.

The following objectives are accomplished with this article.

- Implemented 36 pulse converter to obtain stable dc-link voltage from grid.
- Established PV-battery system and integrated to dc-link to improve the voltage quality at dc-link.
- Design a DTC with two LSTM based ANN controllers to achieve precious response under variable flux region.
- Developed a Space Vector Pulse Width Modulation (SVPWM) on 5L-NPC inverter to obtain t fast and smooth response of speed.
- Developed Modified Invasive Weed Optimization (MIWO) to identify best sector position to achieve quick response during step change in reference speed.

The paper is organized by providing system description in Section-2, design of LSTM controllers in Section-3, control of voltage at dc-link is explained in Section-4. The proposed control of induction motor drive and respective HIL based results are provided in Section-5 and Section-6 respectively. The conclusion is written in Section-7.

2. DESCRIPTION OF THE SYSTEM

The system's proposed configuration is illustrated in Figure 1.The dc-link voltage is established by using 36 pulse converters (by using transformers). A boost converter is utilized in a PV system to serve as both a dc-link and amaximum power point tracker (MPPT) device. The battery bank is integrated to the dc-link through a bidirectional dc-dc converter. During off grid, the battery and PV system can able to supply power to drive. During unbalance voltage at grid causes second frequency oscillation in voltage at dc-link. Hence, the control of bidirectional dc-dc converter is implemented to suppress these oscillations from voltage at d-link. Further, the proposed controller will maintain stable dc-link voltage by regulating charging and charging process of the battery.

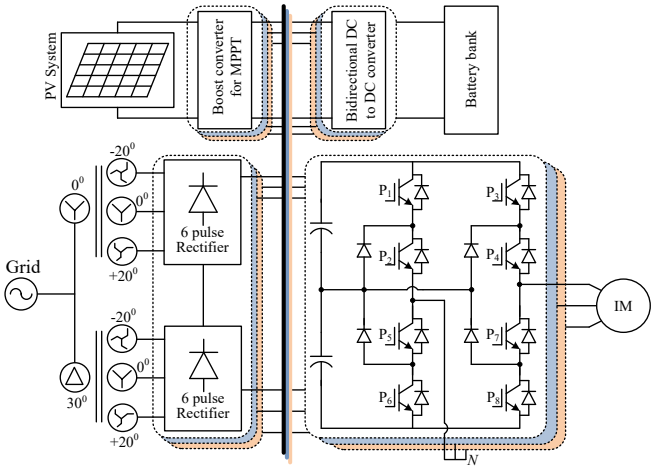

Fig. 1: Proposed configuration of medium voltage drive.

3. LSTM-ANN Controller

Selecting proper controller in a designed control of inverter is very important aspect since it can decide the accuracy of the proposed control method. Due to fixed tuning gains of PI controller, it may not produce proper reference signals quickly in transient periods. The LSTM systemis flexible to adjust their gains according to changes in the system automatically since having machine learning model. Hence, the LSTMsystem can be able to produce accurate reference outputunder any condition. The operation and control of electric drive requires data analysis, processing, verifying and data storage. Hence, ANN based long short term memory (LSTM) algorithm is implemented in this paper from [18-20]. A sophisticated deep learning algorithm is employed to modify the weights of the ANN controller. Generally the signals received from various sections in this Microgrid contain noise. In order to achieve better operation of the drive, the noise signal should be purified. The design of the ANN-based controller unit included the integration of memory cells, as depicted in Figure 2. The LSTM network's internal implementation was developed by utilizing fundamental equations, and its corresponding layout is illustrated in Figure 3. An algorithm based on machine learning (specifically deep learning) has been created to

adjust the weights of the system's neurons in accordance with specified criteria. An unknown noise signal (ns) is also considered since there may be an interfacing magnetic signal in the system due to high voltage and other components. The suppression of these signals is necessary, thus the LSTM block considers the opposite polarity in each element.

$$s_t = f_t \otimes s_{t-1} + \hat{C}_t \times a_t \quad (1)$$

$$h_t = \tanh(s_t) \otimes O_t \quad (2)$$

$$a_t = \sigma(b_a + h_{t-1} \times w_{ah} + X_t \times w_{ax} \mp n_{sa}) \quad (3)$$

$$f_t = \sigma(b_f + h_{t-1} \times w_{fh} + X_t \times w_{fx} \mp n_{sf}) \quad (4)$$

$$O_t = \sigma(b_o + h_{t-1} \times w_{oh} + X_t \times w_{ox} \mp n_{so}) \quad (5)$$

$$\hat{C}_t = \tanh(b_c + h_{t-1} \times w_{ch} + X_t \times w_{cx} \mp n_{sc}) \quad (6)$$

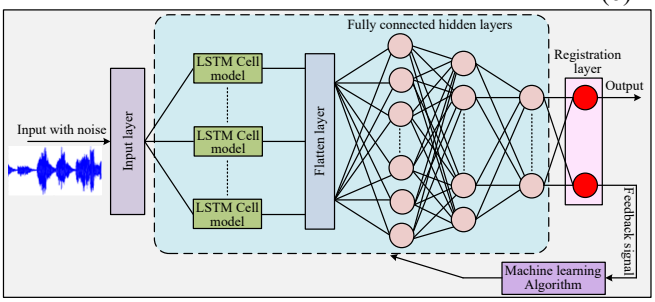

Fig. 2: ANN-LSTM controllers.

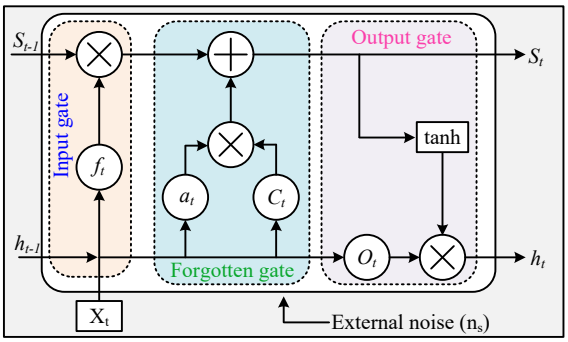

Fig. 3: Single LSTM Model.

4. Control of DC-Link Voltage

From the literature [2], second-harmonic component will be imposed into voltage at dc-link as well as dc-current when inverter needs to supply unbalanced load current at PCC.The electrical torque of the wind coupled generator will have some oscillationswhich results reduce the fatigue life of the shaft. An active filter [2]on dc-side is developed onthe dc/dc converter which paced between the battery bank and dc-link. The battery-associated dc-dc converter has been altered for this objective and is illustrated in Figure 4.

A low pass filter is used to filtered the V_{dc} to obtain the dc-component of voltage(V'_{dc}) then calculated the oscillating component (V_{dco}). Hence, the reference battery current to

produce counter component of the (V_{dco}) is achieved from the PI controller as shown in Fig. 4.

Two PI controllers are used to obtain the resultant reference current of the battery to maintain the constant voltage at dc-link as well as reduce the oscillating component. While producing the counter oscillating component, oscillating component is compared with '0'. The outputs generated from both PI controllers are added to obtain the final reference current (I^*_{bat}) of the battery. The hysteresis loop is implemented to generate the required pulses (Q_1&Q_2) for the bidirectional dc/dc converter from reference and actual currents of the battery bank.

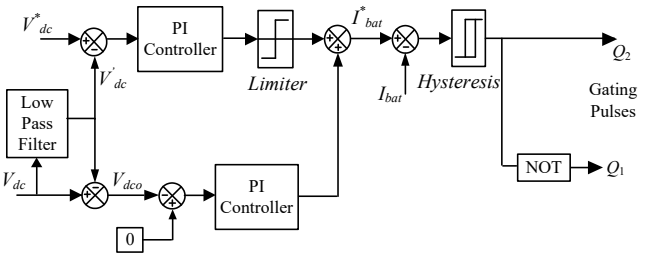

Fig. 4: Proposed control of bidirectional dc-dc circuit.

PROPOSED DTC of INDUCTION MOTOR

In order to provide smooth flux control under prescribe limit, two LSTM controllers used to estimate reference flux and torque signal from motor speed. This can help to break the decoupling effect of the DTC between torque and flux.

The desired pulses are given to SVPWM which is assembled with MIWO technique to achieve the proper pulsing sequence. The generated pulses fromproposed control are given to 5L-NPC inverter to produce AC voltages to drive the induction motor. An LC filter is interface between inverter and motor to further reduce harmonics.

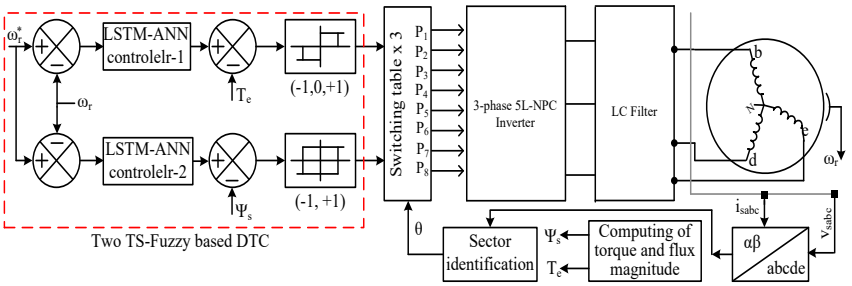

Fig. 5: Proposed Two LSTM based DTC of induction motor with 5L-NPC inverter

A generalized SVPWM of a 5-level (5L) inverter is shown in the Fig. 6by including their respective representations.

Many numbers of switching combinations are possible to generate by the SVPWM technique. Generally, 5L SVPWM can be divided into many 2-level hexagonal systems where each having sevenset of pulses asdepicted in Fig. 7. There is a chance to access many locations (represented by 'L') in the Fig. 7 for any change happened in the system. The reference voltage (V_{ref}) will be rotate in the 5L SVPWM spectrum by passing through each 2-level sub systems. The V_{ref} signal is calculated from V_α& V_β. The below fundamental equations are used to obtain necessary Space Vector Voltage (SV) singles.

$$V_{ref} = \sqrt{V_\alpha^2 + V_\beta^2} \tag{7}$$

$$M = \frac{V_{dc}}{n-1} \tag{8}$$

$$\begin{pmatrix} SV_1 \\ SV_1 \\ : \\ SV_{k-1} \\ SV_k \end{pmatrix} = \begin{pmatrix} V_1.(L-2) \\ V_1.(L-2) + (V_2 - V_1).(1) \\ : \\ V_1.(L-2) + (V_2 - V_1).(k-2) \\ V_1.(L-2) + (V_2 - V_1).(k-1) \end{pmatrix} \tag{9}$$

Here, k[th] support vector is indicated by SV_k.

Total 19 possible combinations for 24 switches during 0-90[0] are listed in Table-1 for 5LNPC inverter which shows in Fig. 1. Remaining combinations for switches during other sectors can be also formulated from these 19 combinations.

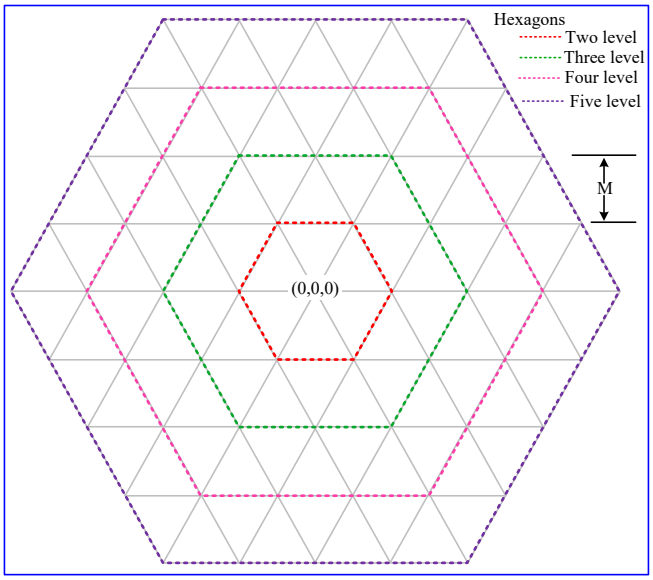

Fig. 6: Hexagonal representation of 5L SVPWM.

Table-1: Switching pattern of pulses between 0 to 90[0]rotation.

No.	Vector.	A-Phase.	B-Phase.	C-Phase
1	0, 0, 0	Null	Null	Null
2	1, 0, 0	$P_{(2, 3, 7, 8)}$	$P_{(10, 11, 14, 15)}$	$P_{(18, 19, 22, 23)}$
3	2, 0, 0	$P_{(1, 2, 7, 8)}$	$P_{(10, 11, 14, 15)}$	$P_{(18, 19, 22, 23)}$
4	3, 0, 0	$P_{(1, 4, 7, 8)}$	$P_{(10, 11, 14, 15)}$	$P_{(18, 19, 22, 23)}$
5	4, 0, 0	$P_{(1, 4, 5, 8)}$	$P_{(10, 11, 14, 15)}$	$P_{(18, 19, 22, 23)}$
6	1, 1, 0	$P_{(2, 3, 7, 8)}$	$P_{(10, 11, 15, 16)}$	$P_{(18, 19, 22, 23)}$
7	2, 1, 0	$P_{(1, 2, 7, 8)}$	$P_{(10, 11, 15, 16)}$	$P_{(18, 19, 22, 23)}$
8	3, 1, 0	$P_{(1, 4, 7, 8)}$	$P_{(10, 11, 15, 16)}$	$P_{(18, 19, 22, 23)}$
9	4, 1, 0	$P_{(1, 4, 5, 8)}$	$P_{(10, 11, 15, 16)}$	$P_{(18, 19, 22, 23)}$
10	1, 2, 0	$P_{(2, 3, 7, 8)}$	$P_{(9, 10, 15, 16)}$	$P_{(18, 19, 22, 23)}$
11	2, 2, 0	$P_{(1, 2, 7, 8)}$	$P_{(9, 10, 15, 16)}$	$P_{(18, 19, 22, 23)}$
12	3, 2, 0	$P_{(1, 4, 7, 8)}$	$P_{(9, 10, 15, 16)}$	$P_{(18, 19, 22, 23)}$

13	4, 2, 0	$P_{(1, 4, 5, 8)}$	$P_{(9, 10, 15, 16)}$	$P_{(18, 19, 22, 23)}$
14	2, 3, 0	$P_{(1, 2, 7, 8)}$	$P_{(9, 12, 15, 16)}$	$P_{(18, 19, 22, 23)}$
15	3, 3, 0	$P_{(1, 4, 7, 8)}$	$P_{(9, 12, 15, 16)}$	$P_{(18, 19, 22, 23)}$
16	4, 3, 0	$P_{(1, 4,5, 8)}$	$P_{(9, 12, 15, 16)}$	$P_{(18, 19, 22, 23)}$
17	2, 4, 0	$P_{(1, 2, 7, 8)}$	$P_{(9, 12, 13, 16)}$	$P_{(18, 19, 22, 23)}$
18	3, 4, 0	$P_{(1, 4, 7, 8)}$	$P_{(9, 12, 13, 16)}$	$P_{(18, 19, 22, 23)}$
19	4, 4, 0	$P_{(1, 4, 5, 8)}$	$P_{(9, 12, 13, 16)}$	$P_{(18, 19, 22, 23)}$

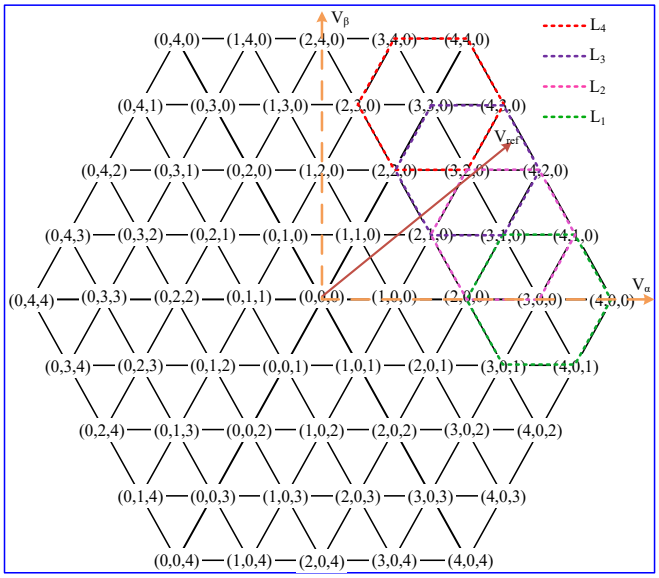

Fig. 7: Space vector representation of 5LSVPWM.

So many possibilities are available in each two level vectors,therefore an efficient optimization algorithm is required to identify the nearest location of vectorto operate the inverter effectively. Hence, a MIWO technique is implemented to capture the best series of the pulses. The MIWO method is a simple and effective technique which inspired by colonizing weed method [ref]. It is already reported in many research papers that the MIWO method is having a high capable in searching the best location under various operating conditions [ref]. Hence, MIWO technique is adopted in this paper in between SVPWM and inverter gating switches to supply the best vector combination. The Cauchy density function utilized in MIWO is characterized by two primary parameters: location and scale. The scale parameter is represented by the standard deviation (σ). The produced new weed is normally distributed over the search space with the varying standard deviation and the mean of the parent weed position as per following representations:

$$\sigma_i = \frac{(w-i)^m}{w^m}(\sigma_{initial} - \sigma_{final}) + \sigma_{final} \qquad (10)$$

$$SV^i_{j+1} = SV^i_j + x\sigma_i \times Cauchy(0,1) \times (SV_{best} - SV^i_j) \qquad (11)$$

Where, $x = \frac{V_{ref}}{V_{dc}} \times \tan\left(\frac{V^i_\beta}{V^i_\alpha}\right)$, 'i' iteration, m is non linear 'w' represents number of parent weeds.

Flowchart representation of implemented MIWO is depicted in Fig. 8.

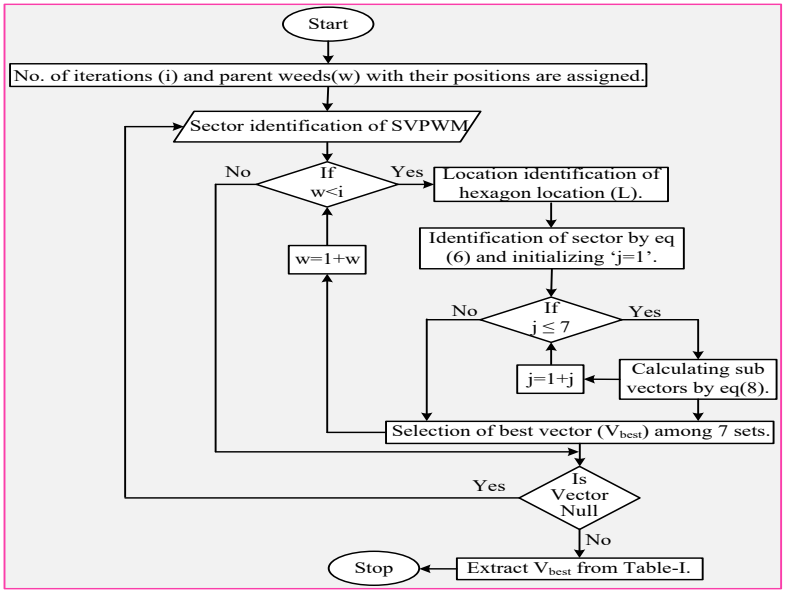

Fig. 8: MIWO-SVPWM of 5L inverter flow chart

5. RESULTS and DISCUSSIONS

The study utilizes real-time simulators (RTS) to improve the system's performance in different scenarios. The laboratory setup involves connecting RTS modules, such as OPAL-RT devices, to establish a hardware-in-the-loop (HIL) configuration. Two OPAL-RT modules are employed to create an HIL environment for testing complex controllers in real-time. The proposed system is implemented in OPAL-RT module 1 (OPAL RT-1), while all the controllers are implemented in OPAL-RT module 2. The system's analog signals are transformed into digital format in order to function as inputs for the controller unit (OPAL RT-2) via data cards. The controller module functions by utilizing the predetermined controllers and produces appropriate switching pulses for the converters employed within the system. The digital pulses are subsequently transformed into analog signals in order to function as input signals for the system via external data cards. Instead of using an oscilloscope, a laptop is utilized to obtain better visualization of the results. Figure 9 illustrates the basic HIL setup consisting of two OPAL-RT modules.

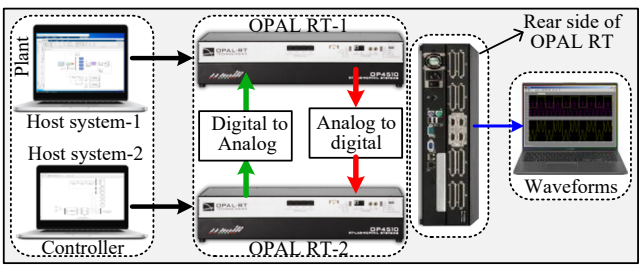

Fig. 9: HIL configuration.

The responses of motor electromagnetic torque, motor/rotor speed and flux trajectory of the induction motor controlled by SVM operated DTC with Two-LSTM logic controllers are presented based on Matlab platform. The response of motor torque along with reference torque is depicted in Fig. 10 during changes at t=1.3 and 1.8sec. During this operation, the

reference torque of the motor set at 5.0Nm from time 1.0sec to 1.3sec; 8.0Nm from time 1.3sec to 1.8sec., and 3.0Nm from 1.8 to 2.0sec. the generated electromagnetic torque of the motor is always followed by reference torque with the help of proposed controller. Respective speed response of induction motor (reference speed (80 rad/s)) is depicted in Fig. 11. From Fig. 10, it is clearly showing that the ripples on torque are minimized. Observed the flux trajectory response from Fig. 12 is very smooth which can helps to operate electrical vehicle smoothly. Flux ripple is observed and noted that it is decreases when ANN controller is in use from trajectory.

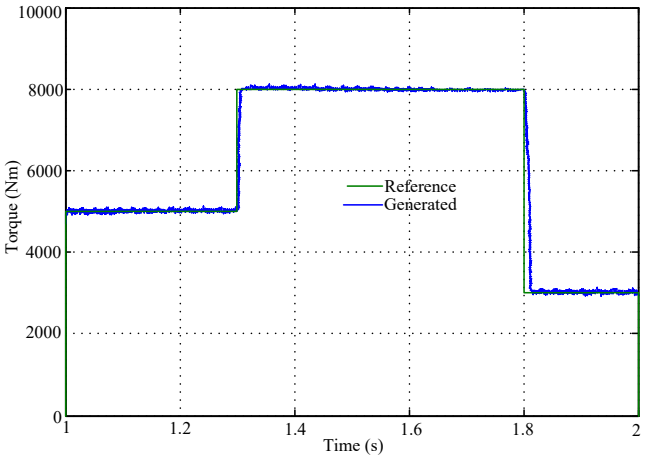

Fig. 10: Torque response of the motor.

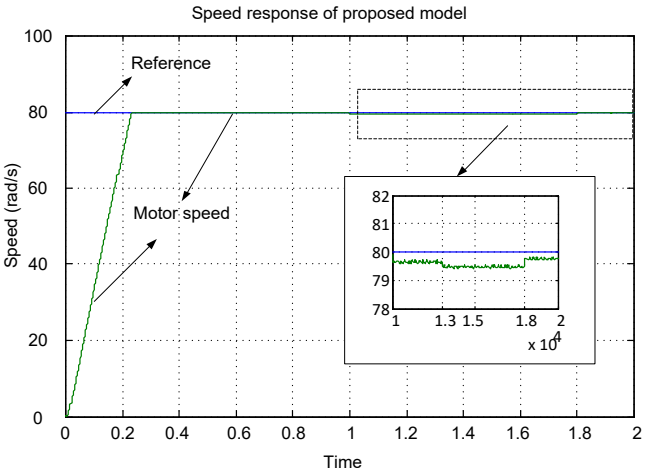

Fig. 11: Speed response of the motor.

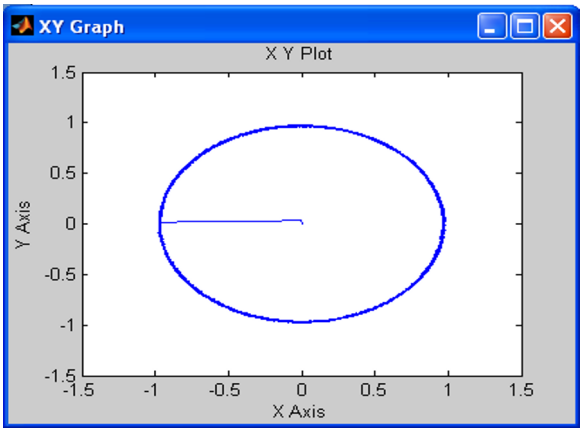

Fig. 12: Stator Flux Trajectory

The inverter's output is examined both with and without employing MIWO, taking into account an abrupt load variation at t=2.50 sec. When 50 percent of load torque of the motor is suddenly changing, the proposed inverter controller is tries to identify proper switching pulses using SVPWM. The time for identification of suitable vector combination is very less with proposed MIWO algorithm, and the rise and dip of the line voltage are less as compared with generalized 5L SVPWM method. Corresponding line voltage response is depicted in Fig. 13 (RMS) with proposed MIWL and generalized SVPWM method. Further the system is tested with and without control of bidirectional dc-dc converter during unbalanced factor of 0.9 in grid voltages. During unbalanced voltages in supply, more oscillations are observed in motor torque which affected on shaft's fatigue life time. The comparable results with and without proposed control of bidirectional converter is shown in Fig. 14.

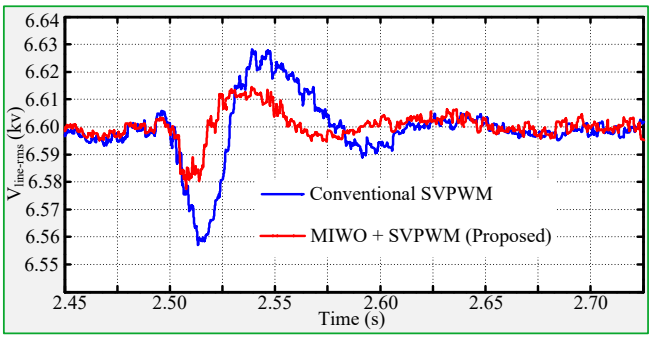

Fig. 13: Response of line to line voltage.

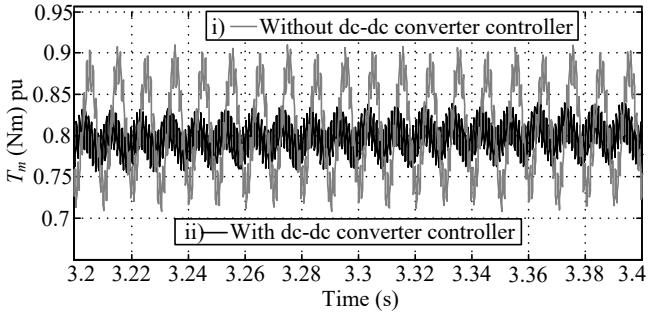

Fig. 14: Oscillations in torque with and without control of dc-dc converter.

Now the system is tested for energy management process. Both wind speed as well as irradiance is changing randomly. However, other loads connected to the system also changed at the same time. Under these conditions, voltages at both dc and ac are varying unknowingly which results poor quality. The changes of load, irradiance and wind speed are considered in this paper which shows in Fig. 15. The battery management system is efficiently operating during this procedure and effectively rectifying the power imbalance between the overall generation and the load. The system's corresponding powers are illustrated in Figure 16. The battery bank charges when there is excess power available and discharges when the load requires more than what is being generated. This behavior can be observed in Figure 17, which illustrates the SoC.

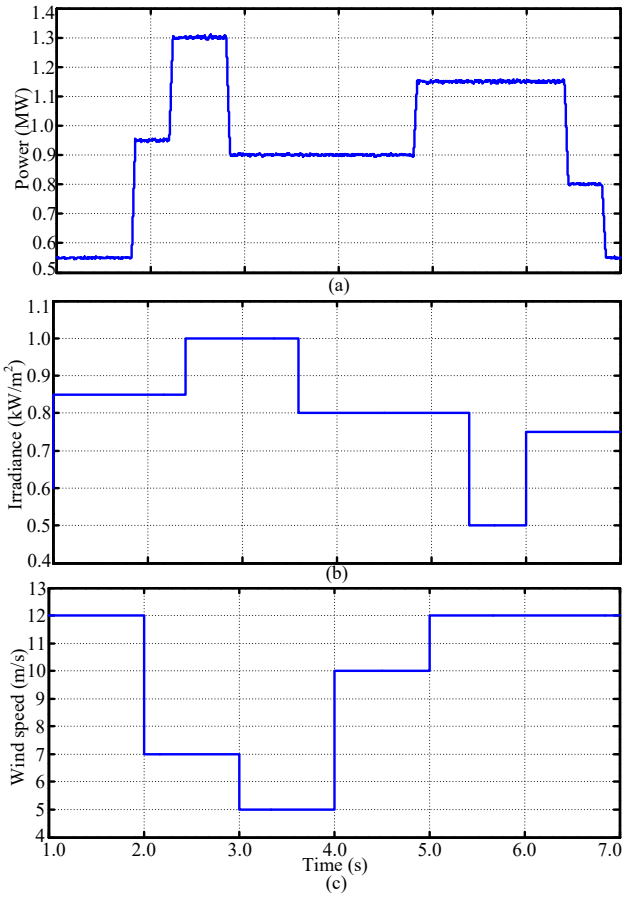

Fig. 15: Various changes in (a) load, (b) irradiance, (c) speed.

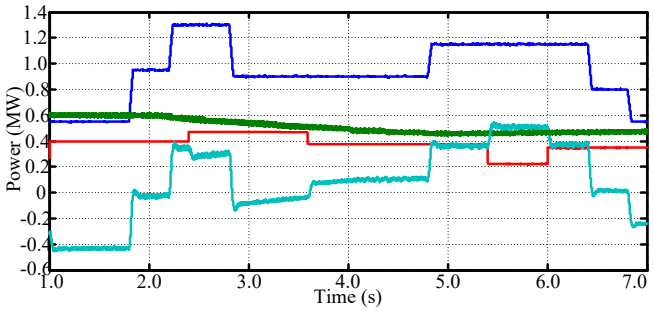

Fig. 16: various powers.

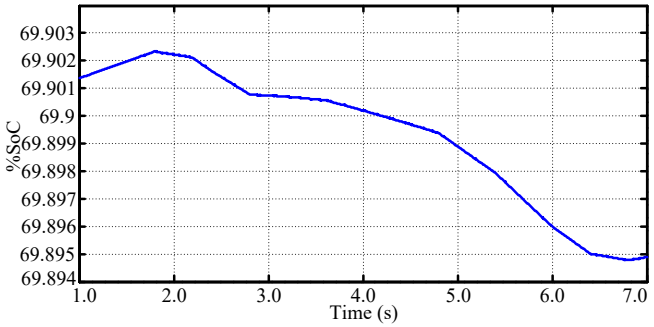

Fig. 17: SoC of the battery bank.

Generally load on the motor varies based on many factors. Hence, the performance of the proposed system is compared with TS-Fuzzy method. Moreover, the response of electromagnetic torque generated by motor is depicted in Fig. 18 under change in reference torque and compared with TS Fuzzy and proposed controller.

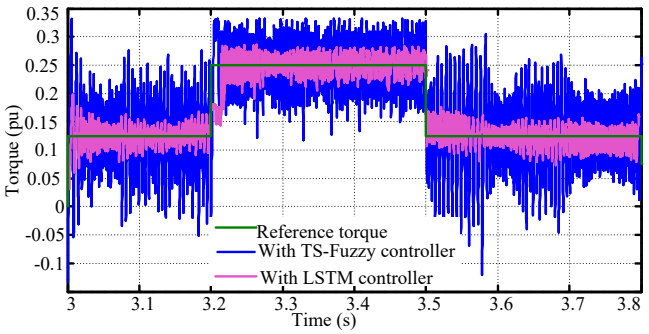

Fig. 18: Response of torque in per unit (pu)

6. CONCLUSION

Two LSTM controllers based DTC of medium voltage induction motor drive is implemented on 5L-NPC inverter for reducing ripples in torque. The MIWO technique is also incorporated to the system for achieving fastest identification of a best vector location to generate accurate pluses according to requirement by the motor. Extensive results are presented in this paper by establishing an HIL with the help of two OPAL-RT modules.

Reference:

[1]. U. R. Muduli and R. K. Behera, "Virtual Vector based SVPWM-DTC for Five-Phase Two-Level VSI fed Induction Motor Drive," *2021 1st International Conference on Power Electronics and Energy (ICPEE)*, 2021, pp. 1-6, doi: 10.1109/ICPEE50452.2021.9358755.

[2]. S. G. Malla, "A review on Direct Torque Control (DTC) of induction motor: With applications of fuzzy", *2016 International Conference on Electrical, Electronics, and Optimization Techniques (ICEEOT)*, 2016, pp. 4557-4567, doi: 10.1109/ICEEOT.2016.7755579.

[3]. B. K. Bose, "Modern Power Electronics and AC Drives, 2001.

[4]. A. P. Biswal and S. Satpathy, "Vector Control of 3-Phase Induction Motor," 2021 1st Odisha International Conference on Electrical Power Engineering, Communication and Computing Technology(ODICON), 2021, pp. 1-4, doi: 10.1109/ODICON50556.2021.9428930.

[5]. C. P. Priyanka and G. Jagdanand, "Multiphase Induction Motor with Different Speed Ratio for Gearless Electric vehicles," 2022 IEEE International Conference on Power Electronics, Smart Grid, and Renewable Energy (PESGRE), 2022, pp. 1-6, doi: 10.1109/PESGRE52268.2022.9715800.

[6]. V. Fireţeanu, A. -I. Constantin and C. Dumitru, "Finite Element Analysis of the Performances of the 3-Phase, 5-Phase, 7-Phase and 9-Phase Squirrel-Cage Induction Motors," 2021 12th International Symposium on Advanced Topics in Electrical Engineering (ATEE), 2021, pp. 1-6, doi: 10.1109/ATEE52255.2021.9425068.

[7]. U. R. Muduli, B. Chikondra and R. K. Behera, "Space Vector PWM Based DTC Scheme With Reduced Common Mode Voltage for Five-Phase Induction Motor Drive," *IEEE Transactions on Power Electronics*, vol. 37, no. 1, pp. 114-124, Jan. 2022, doi: 10.1109/TPEL.2021.3092259.

[8]. S. Ahmad and A. Mishra, "Mathematical Modelling, Simulation and Control of Five-Phase Induction Motor Drives," 2020 International Conference on Emerging Frontiers in Electrical and Electronic Technologies (ICEFEET), 2020, pp. 1-4, doi: 10.1109/ICEFEET49149.2020.9186999.

[9]. C. Pradhan, M. K. Senapati, S. G. Malla, P. K. Nayak and T. Gjengedal, "Coordinated Power Management and Control of Standalone PV-Hybrid System With Modified IWO-Based MPPT," in IEEE Systems Journal, vol. 15, no. 3, pp. 3585-3596, Sept. 2021, doi: 10.1109/JSYST.2020.3020275.

[10]. M. Morawiec and F. Wilczyński, "Control Strategy of a Five-Phase Induction Machine Supplied by the Current Source Inverter With the Third Harmonic Injection," in IEEE Transactions on Power Electronics, vol. 37, no. 8, pp. 9539-9550, Aug. 2022, doi: 10.1109/TPEL.2022.3148526.

[11]. U. R. Muduli, R. K. Behera, K. Al Hosani and M. S. E. Moursi, "Direct Torque Control With Constant Switching Frequency for Three-to-Five Phase Direct Matrix Converter Fed Five-Phase Induction Motor Drive," in IEEE Transactions on Power Electronics, vol. 37, no. 9, pp. 11019-11033, Sept. 2022, doi: 10.1109/TPEL.2022.3167477.

[12]. U. R. Muduli, B. Chikondra and R. K. Behera, "Continuous and Discontinuous SVPWM with Switching Loss Control for Five-Phase Two-Level VSI fed Induction Motor Drive," *2020 IEEE International Conference on Power Electronics, Drives and Energy Systems (PEDES)*, 2020, pp. 1-6, doi: 10.1109/PEDES49360.2020.9379717.

[13]. D. Raja and G. Ravi, "Design of Five Phase Voltage Source Inverter with Time Modulated Switching Technique for Induction Motor Drive," 2019 International Conference on Computation of Power, Energy, Information and Communication (ICCPEIC), 2019, pp. 215-220, doi: 10.1109/ICCPEIC45300.2019.9082354.

[14]. S. He, X. Sui, D. Zhou and F. Blaabjerg, "Torque Ripple Suppression of a Five-phase Induction Motor under Single-phase Open," 2020 IEEE 9th International Power Electronics and Motion Control Conference (IPEMC2020-ECCE Asia), 2020, pp. 3470-3475, doi: 10.1109/IPEMC-ECCEAsia48364.2020.9367677.

[15]. B. Ch, U. R. Muduli and R. K. Behera, "Performance Comparison of Five-Phase Three-Level NPC to Five-Phase Two-Level Voltage Source Inverter," *2018 IEEE International Conference on Power Electronics, Drives and Energy Systems (PEDES)*, 2018, pp. 1-6, doi: 10.1109/PEDES.2018.8707510.

[16]. B. Chikondra, U. R. Muduli and R. K. Behera, “Performance Comparison of Five-Phase Three-Level NPC to Five-Phase Two-Level VSI,” *IEEE Transactions on Industry Applications*, vol. 56, no. 4, pp. 3767-3775, July-Aug. 2020, doi: 10.1109/TIA.2020.2988014.

[17]. Depenbrock M. Direct self-control (DSC) of inverter fed induktion machine. In1987 IEEE Power Electronics Specialists Conference 1987 Jun 21 (pp. 632-641). IEEE. https://doi.org/10.1109/pesc.1987.7077236

[18]. M. Perin, L. A. Pereira, L. F. A. Pereira and G. Nicol, "Estimation of Parameters of Five-Phase Induction Motors Using Step Voltage At Standstill," in IEEE Transactions on Energy Conversion, vol. 36, no. 4, pp. 3491-3501, Dec. 2021, doi: 10.1109/TEC.2021.3085221.

[19]. Siva Ganesh Malla, “Modeling of 5-Phase Induction Motor: A Review”, International Journal of New Technologies in Science and Engineering (IJNTSE), Vol. 8, Issue. 3, pp. 1-8, March. 2022.

[20]. PriyankaMalla, “Novel Control Technique for MPPT of PV Standalone System with TSK Fuzzy controller”, International Journal of New Technologies in Science and Engineering (IJNTSE), Vol. 8, Issue. 8, pp. 1-7, Aug. 2022.

[21]. PriyankaMalla, “TSK Fuzzy Controller for Vector Control of Induction Motor”, International Journal of New Technologies in Science and Engineering (IJNTSE), Vol. 8, Issue. 1, pp. 1-5, Jan. 2022.